TEMPORAL BEHAVIOUR OF PRESSURE IN SOLAR CORONAL LOOPS

K. SASIDHARAN, T. D. SREEDHARAN,* R. PRATAP** and V. KRISHAN
Indian Institute of Astrophysics, Bangalore 560 034, India

(Received 3 May, 1994; in revised form 24 November, 1994)

Abstract. The temporal evolution of pressure in solar coronal loops is studied using the ideal theory of magnetohydrodynamic turbulence in cylindrical geometry. The velocity and the magnetic fields are expanded in terms of the Chandrasekhar–Kendall (C–K) functions. The three-mode representation of the velocity and the magnetic fields submits to the investigation of chaos. When the initial values of the velocity and the magnetic field coefficients are very nearly equal, the system shows periodicities. For randomly chosen initial values of these parameters, the evolution of the velocity and the magnetic fields is nonlinear and chaotic. The consequent plasma pressure is determined in the linear and nonlinear regimes. The evidence for the existence of chaos is established by evaluating the invariant correlation dimension of the attractor D_2, a fractal value of which indicates the existence of deterministic chaos.

1. Introduction

It is well known that loops are the dominant structures in the higher levels of the solar atmosphere. Even though our knowledge of loops has been greatly enhanced in recent years as a result of observations in UV, EUV, and X-ray wavelengths (Foukal, 1978; Levine and Withbroe, 1977; Vaiana and Rosner, 1978), we have little empirical knowledge of the nature of the coronal magnetic field. Therefore a discussion of the relationship between coronal loops and coronal magnetic fields depends heavily on theoretical models.

Coronal loops exhibit a fairly stable and well-configured geometry in spite of the magnetic and velocity field fluctuations in the plasma.Such a steady state is the result of various manifestations of the balance of inertial and magnetic forces. Using the statistical theory of incompressible magnetohydrodynamic turbulence, discussed by Montgomery, Turner, and Vahala (1978), a steady-state model of active region coronal loops was discussed by Krishan (1983a, b). Krishan (1985), Krishan, Berger, and Priest (1988) discussed the dynamics of velocity and magnetic fields in coronal loops. A Vlasov–Maxwell description of coronal loops deriving particle velocity distribution functions in an inhomogeneous plasma has been given by Krishan, Sreedharan, and Mahajan (1991).

Recently Sreedharan *et al.* (1992) have studied the steady state structure of the pressure in coronal loops by representing the velocity and magnetic fields as the superposition of three Chandrasekhar–Kendall (C–K) functions. They discussed

* Permanent address: Department of Physics, Mount Carmel College, Bangalore, 560 052, India.
** Cochin University of Science and Technology, Cochin, 682 022, India.

Solar Physics **157:** 121–133, 1995.

in detail the three-dimensional spatial variation (r, θ, z) of the plasma pressure in coronal loops.

In this paper we extend the results obtained by Sreedharan *et al.* (1992) to include the time dependence of velocity, magnetic field and pressure and study their evolution. Since the evolution equations are coupled and nonlinear, the dependence of their solutions on the initial conditions is expected to reveal chaotic behavior. Towards this end, we investigate in this paper the existence of chaos in the evolution of pressure in coronal loops by studying the power spectrum of the data generated by the solution of the MHD equations and by evaluating the invariant dimension, especially the second order correlation dimension of the attractor D_2 of the system.

In the next section we derive the pressure profile for an incompressible fluid using MHD equations. In Section 3 we give a discussion of the various aspects of dynamics of the system by taking (i) the linear case, (ii) the pump approximation, and (iii) the full set of nonlinear coupled equations and the existence of deterministic chaos by evaluating the second-order correlation dimension which is an invariant parameter of the chaotic system. In this evaluation, we obtain the following information: (a) Is there an attractor and if there exists one, is it regular or strange? (b) Is there only a single attractor or are there more than one? (c) What is the embedding dimension so that in describing nonlinear processes characterized by the set of given equations, what should be the dimensions of the phase space to describe the dynamics of the system. We follow the algorithm that has been proposed by Grassberger and Proccacia (1983). Section 4 deals with the discussion of results of the temporal variations and chaotic behavior of the pressure profile.

2. The Pressure Profile

The pressure profile for an incompressible fluid can be expressed as a function of velocity $\overline{V}$ and magnetic field $\overline{B}$ using MHD equations

$$\frac{\overline{\nabla} P}{\rho} = \frac{(\overline{\nabla} \times \overline{B}) \times \overline{B}}{\rho} - (\overline{V} \cdot \overline{\nabla})\overline{V} - \frac{\partial \overline{V}}{\partial t}\,, \tag{1a}$$

$$\overline{\nabla} \times (\overline{V} \times \overline{B}) - \frac{\partial \overline{B}}{\partial t} = 0\,, \tag{1b}$$

$$\overline{\nabla} \cdot \overline{V} = 0 \quad \text{and} \quad P = nkT\,, \tag{1c}$$

where P is the mechanical pressure, n is the number density of particles, k is Boltzmann's constant, and T is the temperature. The loop plasma is represented by a cylindrical column of length L and radius R. ρ is the mass density and the force due to gravity is neglected. The set of Equations (1a), (1b), and (1c) form a closed set of equations in the variables (V, B, ρ, and T).

Equation (1a) can be manipulated to yield

$$\overline{\nabla}\left(\frac{P}{\rho}+\frac{1}{2}V^2\right)=\left[\frac{(\overline{\nabla}\times\overline{B})\times\overline{B}}{\rho}-(\overline{\nabla}\times\overline{V})\times\overline{V}\right]-\frac{\partial\overline{V}}{\partial t}\,. \tag{2}$$

The velocity field, $\overline{V}$, and magnetic field, $\overline{B}$, can be represented as a superposition of the Chandrasekhar–Kendall functions following Montgomery, Turner, and Vahala (1978). In this study we consider a triple-mode system for the velocity, $\overline{V}$, and magnetic field, $\overline{B}$, written as

$$\overline{V}=\sum_{i=a,b,c,}\lambda_i\eta_i(t)\overline{A}_i\,, \tag{3}$$

$$\overline{B}=\sum_{i=a,b,c,}\lambda_i\xi_i(t)\overline{A}_i\,, \tag{4}$$

$$\overline{A}_{nm}=C_{nm}\overline{a}_{nm}Cr)\,. \tag{4a}$$

C_{nm} is the normalizing constant and $\int\overline{A}^*_{nm}\cdot\overline{A}_{n',m'}\,\mathrm{d}^3r=\delta_{nn'},\ \delta_{mm'}$, where

$$\overline{a}_{nm}(r)=\hat{e}_r\left[\frac{im}{r}+\frac{ik_n}{\lambda_{nm}}\frac{\partial}{\partial r}\right]\psi_{nm}+\hat{e}_\theta\left[\frac{\partial}{\partial r}-\frac{mk_n}{r\lambda_{nm}}\right]\psi_{nm}+$$

$$+\hat{e}_z\left[\frac{\lambda^2_{nm}-k^2_n}{\lambda_{nm}}\right]\psi_{nm}\,, \tag{4b}$$

$$\psi_{nm}=J_m(\gamma_{nm}r)\exp(im\theta+ik_nz)\,,$$

$$\lambda_{nm}=\pm(\gamma^2_{nm}+k^2_n)^{1/2}\,,\qquad k_n=2\pi n/L\,,$$

$$n=0,\mp1,\mp2,\ldots\,,\qquad m=0,\mp1,\mp2,\ldots\,.$$

The functions $\overline{a}_{nm}$ satisfy $\overline{\nabla}\times\overline{a}_{nm}=\lambda_{nm}\overline{a}_{nm}\cdot\gamma_{nm}$ and can be determined from the boundary conditions (Sreedharan *et al.*, 1992). η_i and ξ_i are in general complex.

The dynamics can be described by taking the inner products of the curl of Equations (1a) and 1(b) with $\overline{A}^*_{nm}$ and integrating over the volume. The resulting six complex, coupled, nonlinear ordinary differential equations are

$$\frac{\mathrm{d}\eta_a}{\mathrm{d}t}=\frac{\lambda_b\lambda_c}{\lambda_a}(\lambda_c-\lambda_b)I[\eta_b\eta_c-\xi_b\xi_c/\rho]\,, \tag{5}$$

$$\frac{\mathrm{d}\eta_b}{\mathrm{d}t}=\frac{\lambda_c\lambda_a}{\lambda_b}(\lambda_a-\lambda_c)I^*[\eta^*_c\eta_a-\xi^*_c\xi_a/\rho]\,, \tag{6}$$

$$\frac{\mathrm{d}\eta_c}{\mathrm{d}t}=\frac{\lambda_a\lambda_b}{\lambda_c}(\lambda_b-\lambda_a)I^*[\eta_a\eta^*_b-\xi^*_b\xi_a/\rho]\,, \tag{7}$$

$$\frac{d\xi_a}{dt} = \lambda_b \lambda_c I[\eta_b \xi_c - \eta_c \xi_b] \,, \tag{8}$$

$$\frac{d\xi_b}{dt} = \lambda_c \lambda_a I^*[\eta_c^* \xi_a - \eta_a \xi_c^*] \,, \tag{9}$$

$$\frac{d\xi_c}{dt} = \lambda_a \lambda_b I^*[\eta_a^* \xi_b^* - \eta_b^* \xi_a] \,, \tag{10}$$

where $I = \int \overline{A}_a^* \cdot (\overline{A}_b \times \overline{A}_c)\, d^3r$ and the (n, m) values of the modes (a, b, c) satisfy the condition $n_a = n_b + n_c$ and $m_a = m_b + m_c$. Equation (2) with the representation of $\overline{V}$ and $\overline{B}$ given in Equations (3) and (4) can be manipulated to yield

$$\overline{\nabla}\left(\frac{P}{\rho} + \frac{1}{2}\sum_{i=a,b,c}\sum_{j=a,b,c} \lambda_i \lambda_j \eta_i \eta_j \overline{A}_i \cdot \overline{A}_j\right) = \sum_{\substack{i=a,b,c \\ j=b,c,a}} \lambda_i \lambda_j (\lambda_i - \lambda_j) \times$$

$$\times \left(\frac{\xi_i \xi_j}{\rho} - \eta_i \eta_j\right)(\overline{A}_i \times \overline{A}_j) - \sum_{i=a,b,c} \frac{\partial \eta_i}{\partial t} \lambda_i \overline{A}_i \,. \tag{11}$$

The expansion coefficients η_i and ξ_i can be solved numerically from the dynamical equations (5)–(10) which when substituted in Equation (11) determine pressure as a function of space and time.

3. Dynamical Aspects

The temporal evolution of the pressure is presented for a cylindrical plasma column of length 'L' and radius 'R'. The ratio of the toroidal to poloidal magnetic flux, $\psi(t)/\psi(p)$ is taken as $\frac{1}{10}$. We have chosen the triads a, b, c to represent the largest possible spatial scales and also satisfy the condition $a = b + c$, as $a = (1, 1)$, $b = (1, 0)$, $c = (0, 1)$. Corresponding values of γ_i and λ_i are found to be $\gamma_a R = 3.23$, $\gamma_b R = 3.85$, $\gamma_c R = 3.85$, $\lambda_a R = 3.29$, $\lambda_b R = 3.90$, $\lambda_c R = 3.85$ for a rigid boundary as described in Sreedharan *et al.* (1992). The total energy, E, of the loop plasma in a given configuration (a, b, c) is given by

$$E = 2 \sum_{i=a,b,c} \lambda_i (\eta_i^2 + \xi_i^2) \,.$$

There is no obvious way of fixing the relative magnitudes of the three modes even though we have some estimates of the total energy of a typical loop.

There are two physical situations under which Equations (5)–(10) can be solved analytically. (i) The linear case, (ii) the pump approximation.

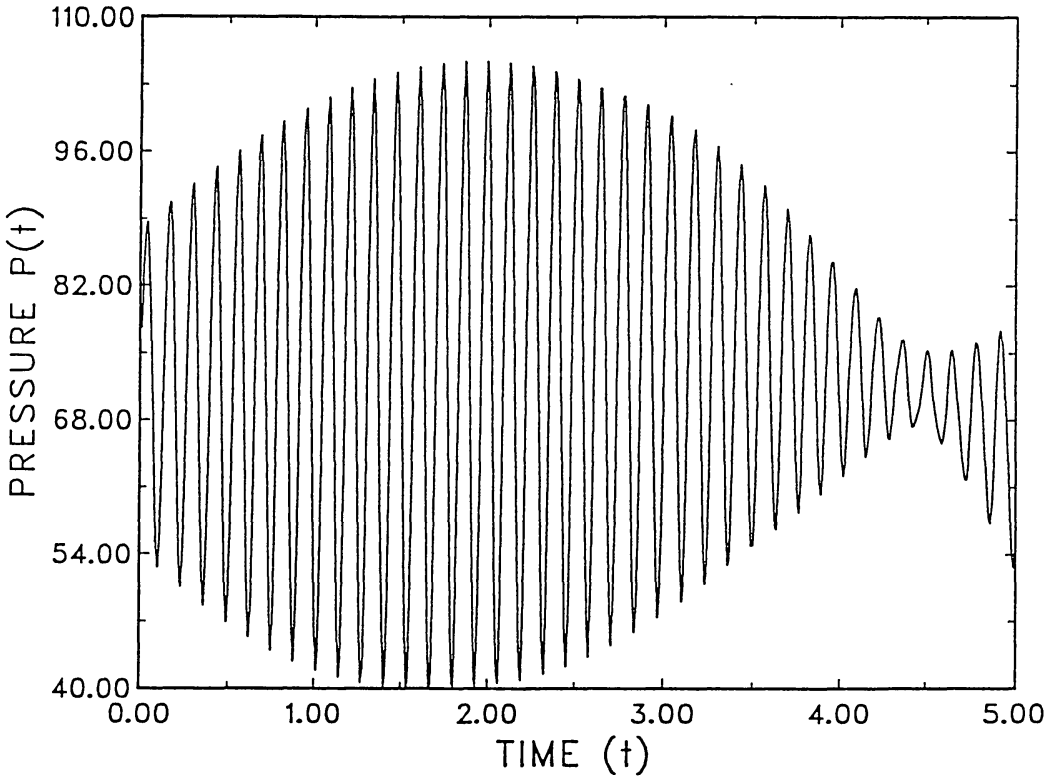

Fig. 1. Temporal evolution of pressure $P(t)$ at an axial point of the coronal loop when the initial values of the velocity and magnetic field coefficients are very nearly equal.

(i) THE LINEAR CASE

Here we study the time evolution of the small deviations of the velocity and magnetic fields from their equilibrium values, i.e., we assume $\eta = \eta_0 + \eta_1$, $\xi = \xi_0 + \xi_1$ and that $\eta_0 = \xi_0$ and $\eta_1 \ll \eta_0$, $\xi_1 \ll \xi_0$ for all modes. Assuming that both $\eta_1(t)$ and $\xi_1(t)$ have time dependence through e^{st}, we can obtain a dispersion relation whose solution is

$$s = \mp i\,|I|\,[\lambda_b^2(\lambda_b - \lambda_c - \lambda_a)^2\,|\eta_{b0}|^2 + \lambda_c^2(\lambda_c - \lambda_a - \lambda_b)^2\,|\eta_{c0}|^2 - \\ -\lambda_a^2(\lambda_a - \lambda_b - \lambda_c)^2\,|\eta_{a0}|^2]^{1/2}\,.$$

Thus the system exhibits marginal stability since the perturbed quantities have sinusoidal oscillations with a period which depends upon the equilibrium values of the fields.

Figure 1 shows the time variation of pressure for the initial values of η_i and ξ_i as follows:

$$|\eta_a| = 1.0\,, \qquad |\eta_b| = 2.0\,, \qquad |\eta_c| = 3.0\,,$$

$$|\xi_a| = 1.1\,, \qquad |\xi_b| = 2.1\,, \qquad |\xi_c| = 3.1\,.$$

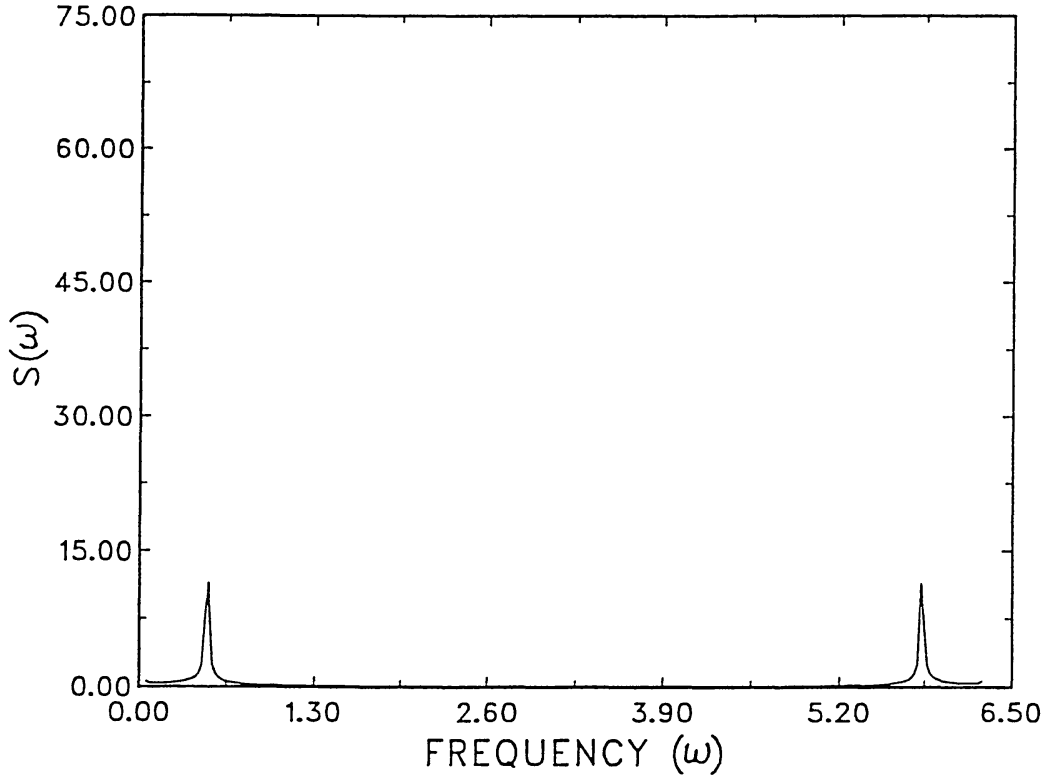

Fig. 2. The power spectrum $[S(\omega) - (\text{constant}) \lim_{T\to\infty} T^{-1} | \int_0^T e^{-i\omega t} P(t)\, dt|^2]$ corresponding to the time variation of pressure shown in Figure 1.

The corresponding power spectrum is shown in Figure 2. This discrete spectrum clearly indicates that the pressure profile has a finite number of frequencies when the magnitude of the velocity and magnetic fields are approximately equal initially. This marginal stability exists only for the time scales for which the linearisation is valid. The *Skylab*, UV and microwave observations do indicate that the loops are in a state of quasi periodic pulsations (Aschwanden, 1987).

(ii) THE PUMP APPROXIMATION

In the pump approximation, one of the three modes is taken to be the strongest. For example, here, since the conservation condition gives $a = b + c$, we can take 'a' to be the dominant mode and call it the pump which shares its energy with the other two modes. The time evolution of the two modes does not produce any significant change in the pump mode, and hence we can neglect all time variations in (η_a, ξ_a). The system of six equations (5)–(10) therefore reduces to four (Equations (5) and (8) are automatically satisfied under the pump approximation since both sides of the equations are vanishingly small) with the additional assumption $\eta_a = \xi_a$ and takes the following simplified form which can be solved analytically:

$$\frac{d\eta_b}{dt} = \frac{\lambda_c \lambda_a}{\lambda_b}(\lambda_a - \lambda_c) I^* [\eta_c^* - \xi_c^*] \eta_a \,, \tag{12}$$

$$\frac{d\eta_c}{dt} = \frac{\lambda_a\lambda_b}{\lambda_c}(\lambda_b - \lambda_a)I^*[\eta_b^* - \xi_b^*]\eta_a \,, \tag{13}$$

$$\frac{d\xi_b}{dt} = \lambda_a\lambda_c I^*[\eta_c^* - \xi_c^*]\eta_a \,, \tag{14}$$

$$\frac{d\xi_c}{dt} = \lambda_a\lambda_b I^*[\xi_b^* - \eta_b^*]\eta_a \,. \tag{15}$$

Complex conjugates of Equation (13) and (15) give

$$\frac{d\eta_c^*}{dt} = \frac{\lambda_a\lambda_b}{\lambda_c}(\lambda_b - \lambda_a)I[\eta_b - \xi_b]\eta_a^* \,, \tag{16}$$

$$\frac{d\xi_c^*}{dt} = \lambda_a\lambda_b I[\xi_b - \eta_b]\eta_a^* \,, \tag{17}$$

and the difference of Equations (16) and (17) gives

$$\frac{d\eta_c^*}{dt} - \frac{d\xi_c^*}{dt} = \frac{\lambda_a\lambda_b}{\lambda_c} I\eta_a^*[\lambda_b - \lambda_a + \lambda_c]\,(\eta_b - \xi_b) \,. \tag{18}$$

A time derivation of Equation (12) can be written as

$$\frac{d^2\eta_b}{dt^2} = \lambda_a^2\,|I|^2\,|\eta_a|^2(\lambda_a - \lambda_c)\,(\lambda_b - \lambda_a + \lambda_c)\,(\eta_b - \xi_b) \,. \tag{19}$$

We have used Equation (18) in writing (19). In a similar manner we can write the equation for $d^2\eta_c/dt^2$.

One can therefore write these equations as

$$\frac{d^2\eta_b}{dt^2} = P_1\eta_b + P_2 \,, \tag{20}$$

$$\frac{d^2\eta_c}{dt^2} = P_1'\eta_c + P_2' \,, \tag{21}$$

where

$$\xi_b = \frac{\lambda_b}{\lambda_a - \lambda_c}(\eta_b - T_b) \,, \qquad I_b = \eta_{b0} - \frac{(\lambda_a - \lambda_c)}{\lambda_b}\xi_{b0} \,,$$

$$\xi_c = \frac{\lambda_c}{(\lambda_a - \lambda_b)}(\eta_c - I_c) \,, \qquad I_c = \eta_{c0} + \frac{(\lambda_b - \lambda_a)}{\lambda_c}\xi_{c0} \,,$$

$$P_1 = \lambda_a^2(\lambda_a - \lambda_b - \lambda_c)^2\,|I|^2\,|\eta_a|^2 \,,$$

$$P_2 = \lambda_a^2\lambda_b(\lambda_a - \lambda_b - \lambda_c)\,|I|^2\,|\eta_a|^2\,I_b \,,$$

$$P_1' = P_1 \,,$$

$$P_2' = \lambda_a^2 \lambda_c (\lambda_a - \lambda_b - \lambda_c) \, |I|^2 \, |\eta_a|^2 I_c \,.$$

Integrating Equations (20) and (21) we get

$$\eta_b = A \, e^{\sqrt{p_1} t} + B \, e^{\sqrt{p_1} t} - \frac{p_2}{p_1} \,,$$

$$\eta_c = Q \, e^{\sqrt{p_1} t} + R \, e^{\sqrt{p_1} t} - \frac{p_2'}{p_1} \,,$$

where A, B, Q, R are to be determined by the initial conditions. This shows that all the four field coefficients, η_b, ξ_b, η_c, ξ_c, exhibit growing and decaying modes. This is understandable since there is an infinite capacity pump mode η_a, ξ_a in the system at the expense of which η_b, ξ_b, η_c, ξ_c are growing. Thus in the case of the pump approximation analytical solutions to the system can be found.

(iii) Chaos in the System

Equations (5)–(10) are a set of six ordinary, first-order differential equations which are highly nonlinear. It may further be realized that the velocity (η_i) and magnetic field (ξ_i) components are motion – characteristic of MHD equations. These equations in principle can be seen as equivalent to one ordinary sixth order differential equation which will manifest all the nonlinearities and therefore may lead to chaotic dynamics. To investigate this aspect we first determine the power spectrum of the system. A broad-band power spectrum is a sure indication of the existence of chaos in the dynamics. An insight into the chaotic system can be obtained by determining the invariant parameters such as correlation dimensions, D_i, Kolmogorov entropies, K_i, Lyapunov exponents, etc., which are all infinite in number. However, it has been shown that of the infinite number of the correlation dimensions and Kolmogorov information entropies, the second-order quantities are the most significant ones, and hence we shall determine D_2 in the present analysis. We shall postpone the determination of K_i and Lyapunov exponents for a later occasion. We follow in this the algorithm which was first proposed by Grassberger and Proccacia (1983) and later developed by Atmanspacher and Schinegraber (1986) and Abraham *et al.* (1986).

Let $\{X_0(t)\}$ be the original time series with the data being taken at constant intervals. These data set can be rearranged so as to get $(d-1)$ additional data sets as

$$X_0(t_1), \ldots, X_0(t_N) \,,$$

$$X_0(t_1 + \Delta t), \ldots, X_0(t_N + \Delta t) \,,$$

$$X_0(t_1 + d\Delta t), \ldots, X_0(t_N + d\Delta t) .$$

We can consider the transpose of the above matrix as consisting of N vectors having d components in a d-dimensional space. The general vector can be written

$$\overline{X}_i = (X_0(t_1), \ldots, X_0(t_i + d\Delta t)) ,$$

where $i = 1, \ldots, N$ and $\overline{X}_i$ is a point in the constructed d-dimensional space. We now evaluate the correlation function

$$C_d(r) = \lim_{N\to\infty} \frac{1}{N^2} \sum_{i,j=1,N} \theta(r - |\overline{X}_i - \overline{X}_j|) ,$$

where θ is the Heaviside function defined as $\theta(x) = 0$ for $x < 0$ and unity for $x > 0$. This implies that if the absolute value of the vector difference $|\overline{X}_i - \overline{X}_j|$ is less than r, we count it as unity, and it is zero if it is greater than r. We then construct the small boxes of side r in phase space and count the vector tips that lie in this box. This is called box counting. It is shown that as r becomes smaller $C_d(r) \sim r^\nu$ so that

$$\log C_d(r) \sim \nu \log r .$$

As $r \to 0$ and $d \to \infty$, ν takes a definite value which is called the second-order correlation dimension and we get

$$D_2 = \lim_{\substack{r\to 0 \\ d\to\infty}} \frac{\log C_d(r)}{\log(r)} .$$

The correlation integral $C(r)$ has to be calculated for several values of r with respect to each particular dimension, d, of the constructed phase space. For each dimension, d, one obtains a $\log C_d(r)$ vs $\log(r)$ curve and the slope, ν, of the linear part of the curve can be obtained using a least-square fit. If the slope, ν, converges towards a finite value for higher values of d, this value is denoted by D_2. When D_2 is an integer, the system is regular and when it is a fractal the system is chaotic.

We have numerically solved Equations (5)–(10) for arbitrary initial values of the field coefficients. The time evolution of pressure at an axial point of the loop for initial values ($|\eta_a| = 4.0$, $|\eta_b| = 7.0$, $|\eta_c| = 10.0$, $|\xi_a = 8.0|$, $|\xi_b| = 11.0$, $|\xi_c| = 14.0$) is shown in Figure 3. The time variation is highly complex. The corresponding power spectrum is shown in Figure 4. The spectrum is fluctuating and broad band, indicating the presence of chaos. A data set of 500 points corresponding to this chaotic evolution of pressure is used to evaluate the information dimension-D_2-by the method described above. In Figure 5, we illustrate the converging slope, and the value of D_2 is found to be 1.732. With the same initial conditions, D_2 was evaluated at a surface point and the slope does not seem to converge to a limiting

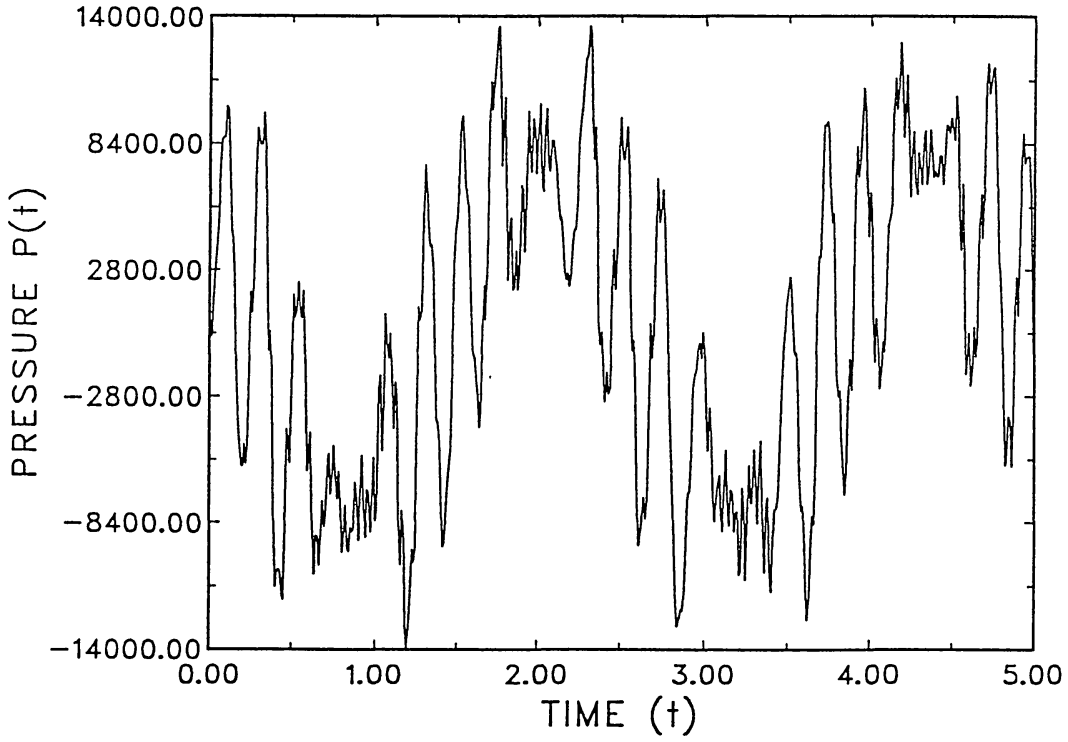

Fig. 3. Time variation of pressure at an axial point of the loop when the initial values of the field coefficients η_a, η_b, η_c are much different from those of ξ_a, ξ_b, ξ_c, respectively.

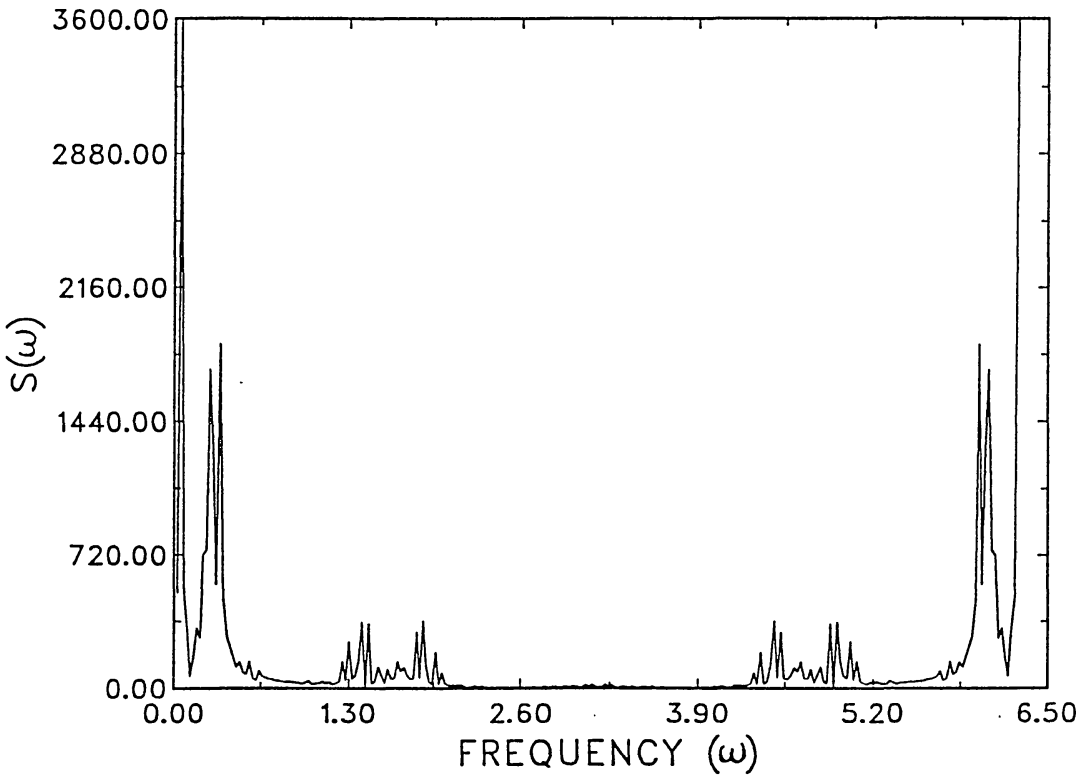

Fig. 4. Power spectrum $S(\omega)$ corresponding to the time variation of pressure shown in Figure 3.

value. This is shown in Figure 6. The fractal value of D_2 evidences the existence of deterministic chaos. In a chaotic regime the system can either dissipate to an attractor stage or can follow a stochastic (random) flow. As the dimension, d, of the constructed phase space increases, the slope, ν, may converge to a limiting value. In this case, the flow will be confined to a geometrical object called an attractor. The converging value of the slope is the dimension, D_2, of the attractor. The dimension of the attractor measures the minimum number of independent parameters needed to describe the system dynamics. In other words if D_2 exists, there is a properly defined dynamical system. The steady increase of slope, ν, with d (Figure 6) evidently shows that it cannot converge and consequently the number of degrees of freedom of the system is increasing. Then the complexity of the system increases and it tends to a more disordered state, indicating that system behavior is stochastic.

4. Conclusion

In the equilibrium state $\eta_a = \xi_a$, $\eta_b = \xi_b$, $\eta_c = \xi_c$. We disturb the system slightly from the equilibrium state and study the time evolution for a small departure from equilibrium. In this case the system is shown to exhibit sinusoidal oscillation with a period which depends upon the initial values of the field coefficients. In other words, when the system is perturbed from a state where the magnetic energy, $B^2/4\pi$, and the kinetic energy, $(\frac{1}{2})mv^2$, are nearly equal, it exhibits marginal stability. The microwave and X-ray observations of coronal loops show quasi-periodic oscillations with time scales ranging from a fraction of a second to tens of minutes (Aschwanden, 1987; Švestka, 1994, and references therein). These oscillations are usually interpreted in terms of magnetohydrodynamic waves in a loop plasma (Roberts, Edwin, and Benz, 1984). The observed power spectrum of pulsations actually exhibits a more complex behaviour (e.g., Figure 1(d) of Švestka, 1994) which appears quasi-periodic only if we ignore finer variations. Thus quasi-periodic behaviour is expected only near equilibrium as is shown in our studies and the linear wave analysis studies. Under large departures from equilibrium, a loop will show a complex temporal structure which can only be described in terms of objects with fractal dimensions in the phase space of the velocity and magnetic field. Coronal loops being continuously subjected to external forcing through their foot points and through their interaction with neighbouring regions are most likely to be in a chaotic state of pressure fluctuations. Therefore, when there are large deviations from equilibrium, i.e., for initial values of η_a, η_b, η_c much different from those of ξ_a, ξ_b, ξ_c, respectively, the system is nonlinear and so is the corresponding time evolution of the pressure. In this case each individual mode becomes distinct, stronger and mode-mode interaction can take place. In the pump approximation case, since the variation of the strongest mode is negligible when compared with other modes, the interaction is between less number of modes of oscillations, and the system showed oscillatory behavior, whereas the chaotic behaviour is caused

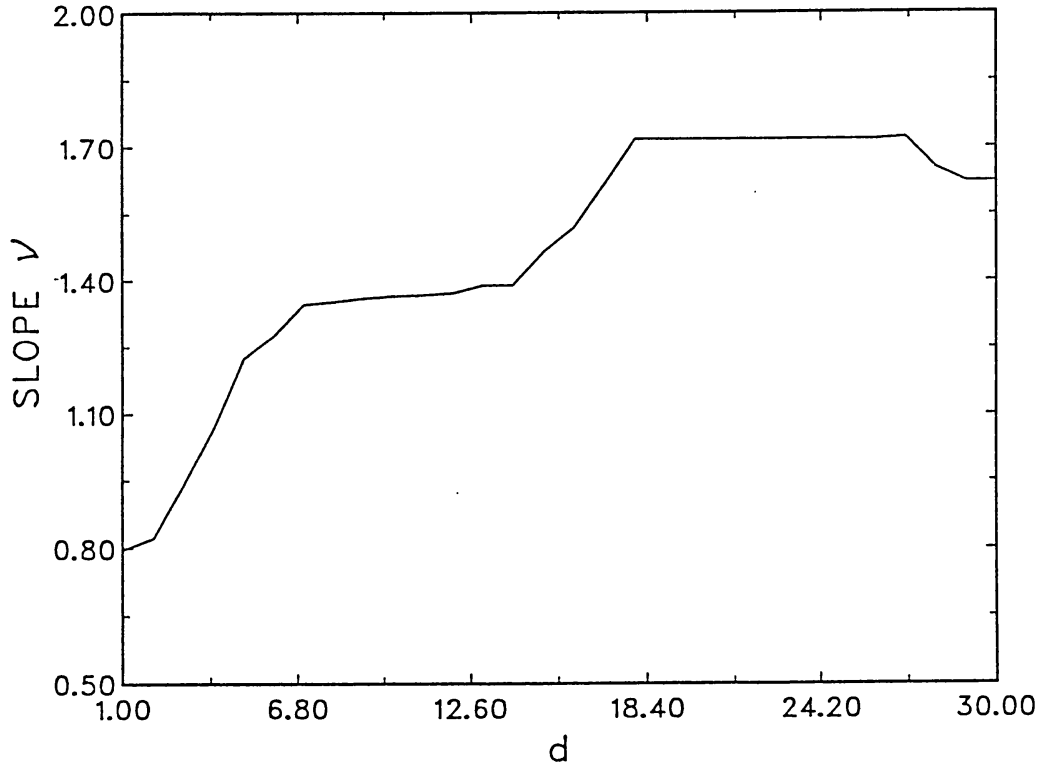

Fig. 5. The slopes (ν) of the linear part of the $\log C_d(r)$ vs $\log(r)$ curves, obtained using least-squares fits, are plotted against the dimension d of the constructed phase space. The two asymptotic values of the slopes are 1.39 and 1.73. This corresponds to the chaotic evolution of pressure at an axial point of the loop.

by the superposition of more than two modes of oscillation and is due to strong nonlinear coupling between them, as is indicated in the nonlinear case above. This fact is evident in the evaluation of D_2. Figure 5 shows the determination of D_2 at an axial point. It is interesting to note that we get two asymptotic values one at 1.39 and the other at 1.73. This could be interpreted as the existence of two strange attractors with embedding spaces of dimension 7 and 18 and the trajectory can land up on either of these attractors. The fact that these are strange attractors (because of fractal dimension) the trajectories could jump from one to the other. This clearly shows the complexity of the situation. The curve of slope ν vs dimension d at $r = R$ does not show any saturation, and the curve is more or less centered on the 45° line, showing the presence of randomness or white noise as shown in Figure 6. Thus as we proceed from the axis towards the surface, the dynamics show the development of strange attractors ending up in complete randomness.

In Figures 5 and 6, even though the initial values of ξ_s and η_s are the same, those of pressure, P, at ($r = 0$, $t = 0$) and at ($r = R$, $t = 0$) are not same. This difference in Figures 5 and 6 is due to the different initial values of pressure at axial and surface points. The transition from a strange attractor state to randomness requires a much finer analysis, which will be investigated on a future occasion. In conclusion, the time scale over which the system is stable or otherwise can

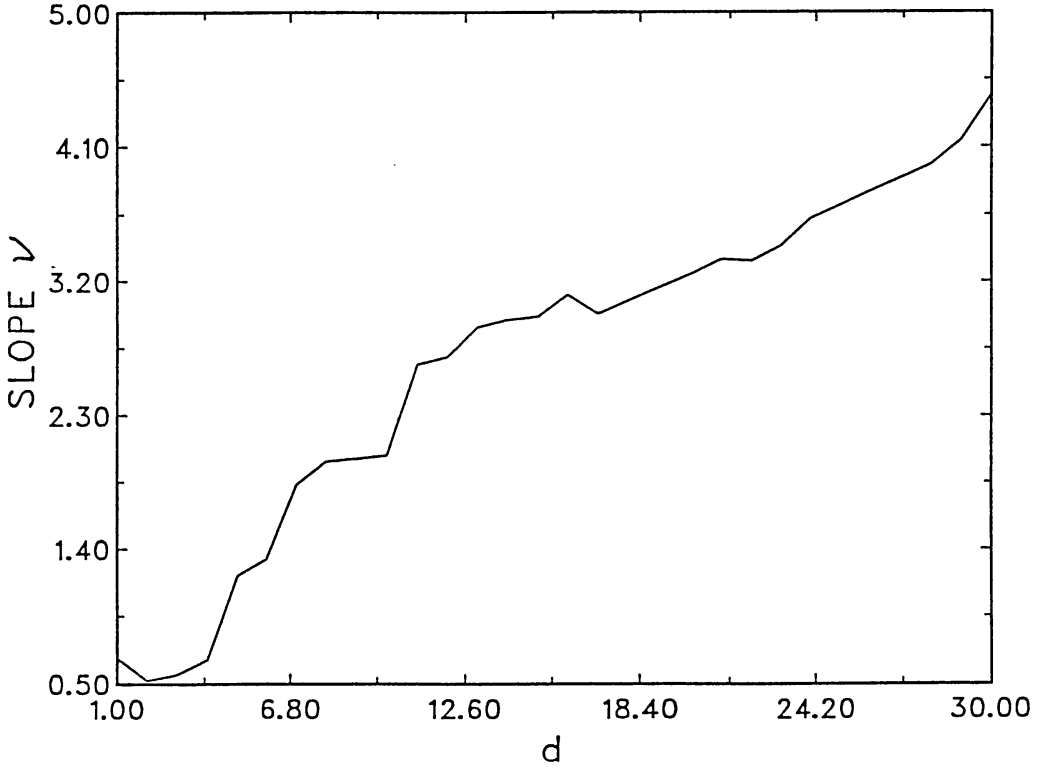

Fig. 6. Corresponding to the chaotic time evolution of pressure at a surface point of the loop, the slopes (ν) of the linear part of the $\log C_d(r)$ vs $\log(r)$ curves are plotted against the dimension d. The slopes do not converge to any limiting values.

be inferred only by evaluating the Lyapunov constants, which are sensitive to the initial conditions. Inverting the problem, by specifying the Lyapunov constants, one can possibly evaluate the class of initial states which can give the observed lifetime of the loops.

References

Abraham, N. B. *et al.*: 1986, *Phys. Letters* **A114**, 217.
Aschwanden, M. J.: 1987, *Solar Phys.* **111**, 113.
Atmanspacher, H. and Scheingraber, H.: 1986, *Phys. Rev.* **A34**, 253.
Foukal, P. V.: 1978, *Astrophys. J.* **223**, 1046.
Grassberger, P. and Procaccia, I.: 1983, *Phys. Rev. Letters* **50**, 346.
Krishan, V.: 1983a, *Proceedings of the Spring College on Radiation in Plasmas*, Trieste, Italy.
Krishan, V.: 1983b, *Solar Phys.* **88**, 155.
Krishan, V.: 1985, *Solar Phys.* **95**, 269.
Krishan, V., Berger, M., and Priest, E. R.: 1988, in R. C. Altrock (ed.), *Solar and Stellar Coronal Structures and Dynamics*, National Solar Observatory.
Krishan, V., Sreedharan, T. D., and Mahajan, M.: 1991, *Monthly Notices Roy. Astron. Soc.* **249**, 596.
Levine, R. H. and Withbroe, G. L.: 1977, *Solar Phys.* **51**, 83.
Montgomery, D., Turner, L., and Vahala, G.: 1978, *Phys. Fluids* **21**, 757.
Roberts, B., Edwin, P. M., and Benz, A. O.: 1984, *Astrophys. J.* **279**, 857.
Sreedharan, T. D., Sasidharan, K., Satyanarayanan, A., and Krishan, V.: 1992, *Solar Phys.* **142**, 249.
Švestka, Z.: 1994, *Solar Phys.* **152**, 505.
Vaiana, G. S. and Rosner, R.: 1978, *Ann. Rev. Astrophys.* **16**, 393.